TRANSVERSALLY INJECTED SYNTHETIC JETS FOR WALL TURBULENCE CONTROL

M. Cannata, G. Iuso
Politecnico di Torino (I), Dipartimento di Ingegneria Aeronautica e Spaziale

Abstract

Fully developed turbulent channel flow has been forced by means of transversal forcing operated with arrays of adjacent synthetic jets. The main flow has been controlled injecting groups of synthetic jets tangentially to the horizontal upper channel wall and perpendicularly to the mean flow itself. The effects of the forcing at two different Reynolds numbers have been investigated varying the forcing frequency and the synthetic jets arrays configuration. Skin friction reduction and near wall turbulence attenuation have been observed up to long distance (X=153H) downstream from the forcing section. In the spanwise direction the effects of the forcing is persistent up to a distance ΔZ/B from the vertical wall of injection, that depend from the Reynolds number. Higher level of drag reduction and turbulence attenuation are evidenced at lower Reynolds number.

1 Introduction

Drag reduction is one of the most important goal in the aeronautical field due to the possibility of saving fuel especially for civil transport aircraft. A consistent number of techniques have been proposed and some of them are particularly promising. Transversal forcing on a wall bounded turbulent flow has been demonstrated to be very effective because is able to give rise at consistent levels of drag reduction. The disturb can be introduced in different ways and both experimental and numerical investigations have confirmed the effects of such a forcing on wall turbulent flows.

Spanwise periodic wall oscillations has been considered by many authors for the control of wall turbulence for both external and internal flows. The response of wall-flow turbulence to high-frequency spanwise oscillations was investigated by Jung et al.[1] performing direct numerical simulations of a planar channel flow subjected to oscillatory spanwise cross-flow. Spanwise oscillations at $T^+=100$ produced 40% of drag reduction and comparable attenuations in all three components of turbulence intensities as well as the turbulent Reynolds stress were observed. An experimentally investigation was performed by Laadhari et al. [2] to study the response of a turbulent boundary layer developing on a flat plate to a local spanwise oscillation of the wall. The non-dimensional oscillation frequency f^+ was varied between 0.0033 and 0.0166 and the wall motion amplitude ΔZ^+ was maintained constant and equal to 160. The turbulent fluctuations were decreased almost along the whole boundary layer as the forcing frequency increased. By means of hot wire anemometry and flow visualizations Choi and co-authors [3] demonstrated experimentally the efficiency of the wall spanwise oscillations to control the wall turbulence observing 45% of drag reduction within five boundary layer thicknesses downstream the start of wall oscillation. The mechanisms that lead to turbulent drag reduction in the case of spanwise-wall oscillations were investigated by Choi [4] analyzing experimental data of the near wall structure of a turbulent boundary layer modified by transversal wall motion. The author attributed the modification of the mean velocity profile (reduced mean gradient near the wall and logarithmic region shifted upwards) mainly to

the negative spanwise vorticity created by the oscillating wall. The near wall structure modification in a turbulent boundary layer under the effect of transversal oscillating wall was experimentally studied by Iuso et al. [5]. The low speed streaks behaviour was statistically analyzed observing particle image velocimetry velocity fields in a plane parallel to the wall. The observed reduction in turbulence activity (velocity variance and Reynolds stress) was accompanied by an increase of the averaged low speed streaks width and spacing. Moreover also a reduction of the low speed streaky strength was observed. Transversal forcing can also be applied with other techniques. Transverse travelling wave are able to suppress turbulence production altering substantially the near wall structures as reported by Du et al. [6], [7]. The authors generated travelling by means of a spanwise force confined in the viscous sublayer leanding to more than 30% of drag reduction. Lorentz force has been also introduced to control turbulent boundary layer. Du and Karniadakis [6], Bergher et al. [8] performing direct numerical simulation used spanwise–wall oscillations generated by Lorentz force and confirmed the reduction of wall shear stress. Karniadakis and Choi [9] reviewed possible mechanisms responsible for turbulent drag reduction and corresponding near wall modifications when transversal motion forced a wall turbulent flow by passive means, e.g. riblets, or by active techniques such as wall oscillations or transverse travelling-wave excitations.

Periodic oscillating flows can also be introduced considering synthetic jets as a forcing. These flow fields were introduced by different authors, Smith and Glezer [10], Gelzer and Amitay [11] among others, are zero net mass flow rate in nature and are generated by an oscillating surface under an orifice. At the orifice exit the surface periodic oscillations give rise to periodic emission of vortex ring or 2D vortices according to the orifice geometry (circular or 2D slit). Near the orifice, up to some orifice transversal size, the flow periodically invert the motion direction according to the blowing or suction phase imposed by the surface oscillations. Further downstream along the jets axis, the flow is always directed downstream exhibiting characteristics similar to those of continuous jets. Different applications of such oscillating fluidynamic fields are present in the literature ranging from skin friction reduction, delay separation, jet vectoring, mixing control, etc. In the case of wall turbulence control Park et al.[12] forced a turbulent boundary layer developing on a flat plate using synthetic jet issuing from a thin spanwise slot. The effect of forcing frequency and jet orientation were investigated evidencing a decreases of near wall-region velocity downstream of the slot. Iuso and Di Cicca [13] used couples of convergent synthetic jets injected perpendicularly to a fully developed turbulent channel flow. For values of the forcing frequency f^+ ranging between 0.0082 and 0.0287 simultaneous reduction of wall shear stress and wall turbulent fluctuation were observed.

In this paper the authors present results related with an experimental investigation performed in a fully developed turbulent channel flow forcing the main flow with a large scale manipulating technique. Array of circular adjacent synthetic jets were used injecting the forcing flow transversally to the channel flow and tangentially to one horizontal channel wall. The effects of the oscillation frequency and those of the synthetic jets array configurations are presented for two Reynolds numbers.

2 Experimental set up

The experiment was carried out in a channel characterized by length equal to 8m and a cross-section having height 2H and width B respectively equal to 20mm and 280mm. The settling chamber and the convergent were positioned upstream at the inlet of the channel and a centrifugal blower provided to feed the channel flow. The test section was positioned 5 meters downstream the channel inlet, equivalent to 135 hydrodynamic diameters, to guarantee fully developed turbulence in the channel. The upper wall of the test section was movable in the spanwise direction for the probes positioning transversally respect to the main

flow in order to investigate the transversal organization of the flow.

The system cylinder-oscillating piston was the main part of the actuators. Commercial engines of aircraft model were considered for the realization of the synthetic jets actuators. On the top part of each cylinder a small plexiglas cylinder was mounted in order to feed ten orifices on vertical wall of the channel through pneumatic tubes. The internal diameter of the orifice exit was equal to 2mm. Two groups of synthetic jets were connected with two independent actuators L and R operating in opposition phase. The two independent groups of synthetic jets were one adjacent to the other in such a way that opposition phase operation of the two piston gave also rise in the streamwise direction to a modulation of the forcing. The two forcing groups was positioned on the vertical wall only on one side of the channel and only tangentially to one horizontal wall, as reported in figure1. To investigate also on the wall opposite to the injection, we change the injection on the other horizontal wall and performed measurements always on the same wall. The configuration of the injection was varied according to the number of orifice connected with each actuator. In figure 1 the sketch of the channel and of the actuators is shown.
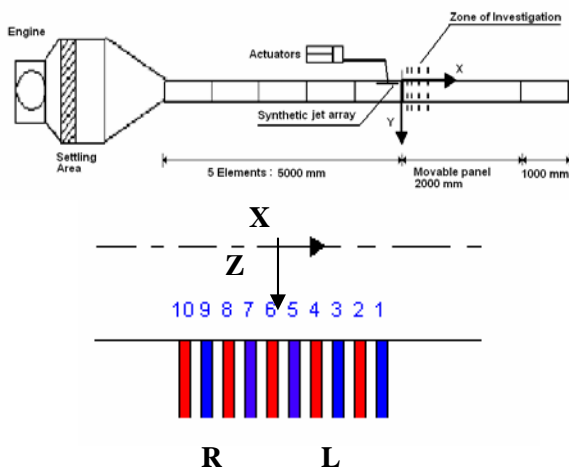
Hot wire anemometry was used for the instantaneous wall shear stress measurements. The sensor probe operated with an overheat ratio equal to 1.7 and calibrations were performed in situ. A fourth order polynomial was adopted to fit the experimental calibration data to linearized via software the probe voltage signal. Two set of measurements were performed, the first one for the statistical analysis aimed at the evaluations of mean and standard deviations of the wall shear stress. The second set of measurements were long time series for the evaluation of spectra, the wall events identification and the autocorrelation function calculation. The acquisition time, equal to 200 seconds was maintained constant for both sets while the sampling frequency was different, 2kHz and 12kHz were respectively adopted for the first and the second set. Synthetic jets axial velocity distributions were also investigated using a total pressure probe mounted on the opposite wall respect to that of the jets injection. This investigation was performed in still air conditions and the ambient pressure was considered as reference pressure.

3 Results and discussion

The non-dimensional axial velocity distributions of some synthetic jets arrays are reported in figure 2. Remark that measurements were performed in still air condition in the channel. The reference velocity to made dimensionless the velocity distributions was the one at the channel centreline, U_c=5.4m/s, corresponding to the experimental conditions of the lower Reynolds number. The velocity measurements were carried out in the centre of only one group (L or R). The injection was located at Z/B=0.5 from only one side of the channel as shown in figure 1.

The axial velocities increase in the neighbour of the orifice exit and the maximum values and their locations depend on the array configuration. Below specific values of Z/B the velocity tends to become negative and are not reported in the diagram.

Fig.1 Channel and synthetic jet array sketches
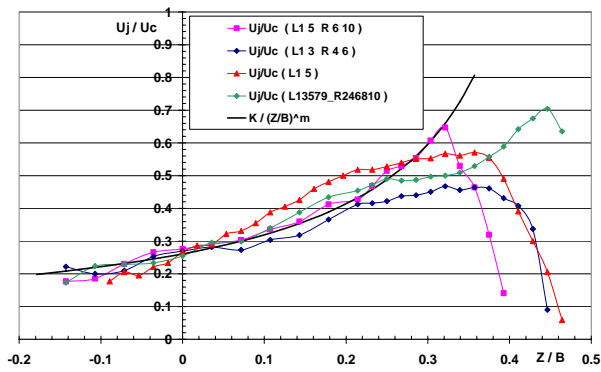
Fig. 2 Axial velocity distribution Channel and synthetic jet array

Fig. 3 Effect of synthetic jets configuration. Mean skin friction percentage variations. X=38H. Z=0.357B. Re_τ=180

After the maximum value, each velocity distribution gives evidence of a decay behaviour that follows approximately the typical decay law k/x^m of isolated synthetic jets [10],[11]. The curve corresponding to this law is also reported in the figure for k=0.14 and m=0.9 The highest peak value is observed for configuration L_{13579} R_{246810} that give rise to $U_j/U_c \approx 0.7$.

In figure 3 and figure 4 the percentage variations of the mean skin friction and of the rms values of the wall shear stress fluctuations, as function of the non dimensional forcing frequency fH/U_c, are shown. Results are referred at Reynolds number, based on the friction velocity and the half channel height, equal to 180 and for streamwise and spanwise positions equal respectively to X=38H and Z=0.357B. The array configurations of synthetic jets investigated are the same tested for the axial velocity distributions reported in figure 2. It can be observed from both figures, that each configuration presents a window of frequencies whose values give rise to drag reduction and to turbulent fluctuations attenuation. The amplitude of the windows and the peaks of reduction depend on the array configuration.

It is evident that for a simultaneous reduction of both drag and turbulent fluctuations, the most efficient forcing configuration is $L_{1\ 5}\ R_{6\ 10}$. This array configuration highlights a peak of drag reduction equal to 22% and a peak of skin friction fluctuations equal to 16% obtained for fH/U_c=0.0074 and fH/U_c=0.011 respectively.
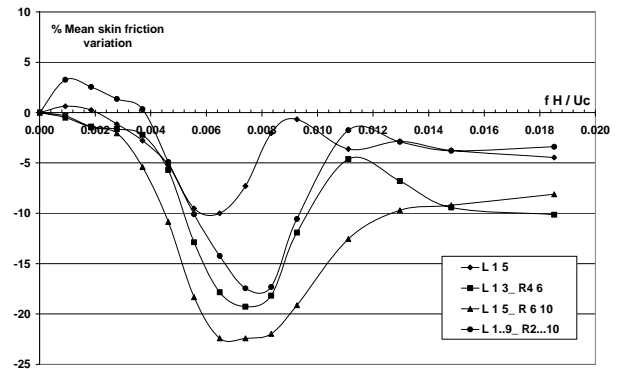
These last non-dimensional frequencies correspond to f=4Hz and f=6Hz in terms of dimensional frequencies. Slightly higher fluctuations reduction are observed for the configuration $L_{1\ 3}\ R_{4\ 6}$ for which the peak of reduction is equal to 16.8% for higher frequency equal to 0.0148.
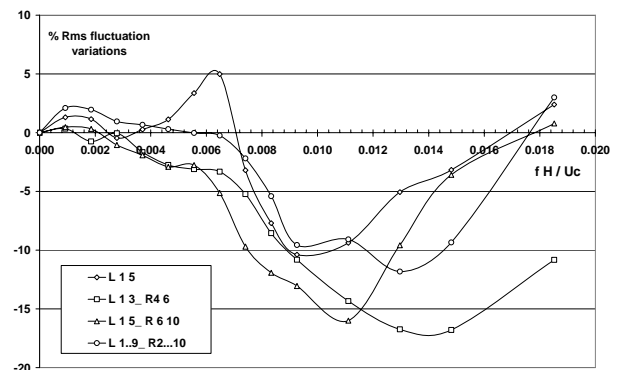
Fig. 4 Effect of synthetic jets configuration. Skin friction rms fluctuations percentage variations. X=38H. Z=0.357B. Re_τ=180

Analogous results relatively to Reynolds number equal to 370 and for the same positions X/H and Z/B, are reported in figure 5 and figure 6. The configurations considered were some of those investigated at lower Reynolds number ($L_{1\ 3}\ R_{4\ 6}$ and $L_{1\ 5}\ R_{6\ 10}$) and a new one: $L_{1\ 3}\ R_{8\ 10}$. At higher Reynolds number the effects of the forcing are similar to those observed at the lower one.
The main differences evidenced respect to the lower Reynolds number, are related with the

lower levels of reductions especially for the turbulent fluctuations.
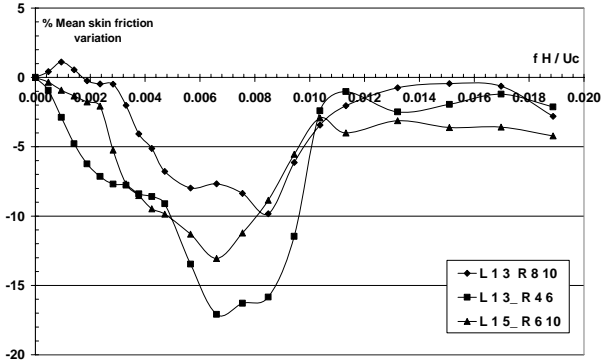
Fig. 5 Effect of synthetic jets configuration. Mean skin friction percentage variations. X=38H. Z=0.357B. Re$_\tau$=370

At Re$_\tau$=370 the highest drag reduction is of the order of 17% obtained for the configuration is L$_{1\ 3}$ R$_{4\ 6}$ while the highest turbulent fluctuations reduction is equal to 5% obtained with the configuration L$_{1\ 3}$ R$_{8\ 10}$. The peak of drag reduction at Re$_\tau$=370 is evidenced for a dimensional forcing frequency nearly double (f=8Hz) respect to that of lower Reynolds number.
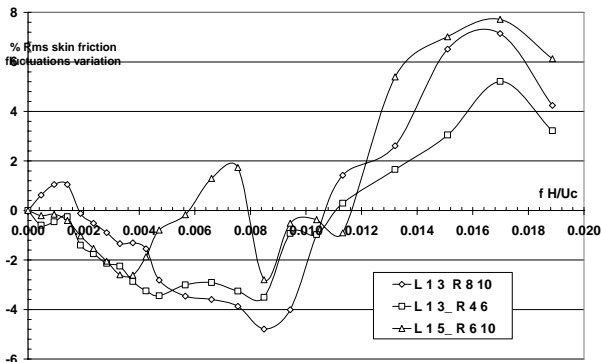
Fig. 6 Effect of synthetic jets configuration. Rms skin friction fluctuations percentage variations. X=38H. Z=0.357B. Re$_\tau$=370

This last dimensional frequency in terms of fH/U$_c$ is nearly the same evidenced at Re$_\tau$=180 for the highest drag reduction. In the following will be shown results derived from the analysis focused on the array configurations that for the two different channel flow conditions gave rise to the highest drag reductions, namely the

configuration L$_{1\ 5}$ R$_{6\ 10}$ for Re$_\tau$=180 and the configuration L$_{1\ 3}$ R$_{4\ 6}$ for Re$_\tau$=370. In figure 7 and figure 8, for the lower Reynolds number, the percentage variations of the mean skin friction and of the root mean square values of the fluctuations are displayed as a function of the non dimensional forcing frequency. The results are referred for different streamwise distances from the injection section. The spanwise position was maintained fixed and equal to Z=0.357B.
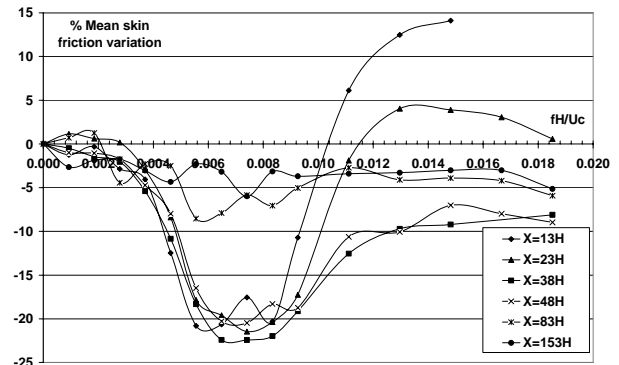
Fig. 7 Effect of forcing frequency. Mean skin friction percentage variations along the streamwise direction. Configuration L$_{15}$ R$_{6\ 10}$ Z=0.357B. Re$_\tau$=180
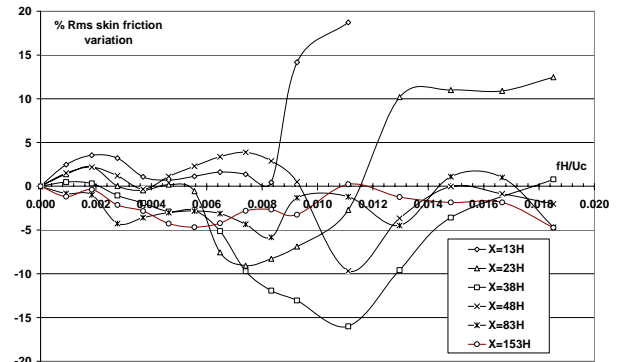
Fig. 8 Effect of forcing frequency. Rms skin friction percentage variations along the streamwise direction. Configuration L$_{1\ 5}$ R$_{6\ 10}$ Z=0.357B. Re$_\tau$=180

The effects of the forcing highlight the highest drag reduction in the streamwise direction in the range 13<X/H<48. At longer distances X/H=83 and X/H=153 the reductions are still persistent but the trend is to recover the undisturbed flow conditions. Also the turbulent fluctuations reflect a similar behaviour but the frequency range that give rise to attenuations is shifted

towards higher values respect to that involved for the drag reduction. Best turbulent fluctuation reductions are shown for X=38H and for fH/U_c=0.011. In figure 9 and figure 10 results similar to the previous ones are reported for Re_τ=370. It is confirmed that along the channel lower drag reductions and lower turbulent fluctuations attenuations characterise the behaviour at higher Reynolds number. The maxima mean skin friction reductions take place between X/H =23 and X/H=48 where, for $0.005 < f H/U_c < 0.009$, assume values in the range 8% ÷17%. The recover of the undisturbed flow conditions appears from X/H=48.
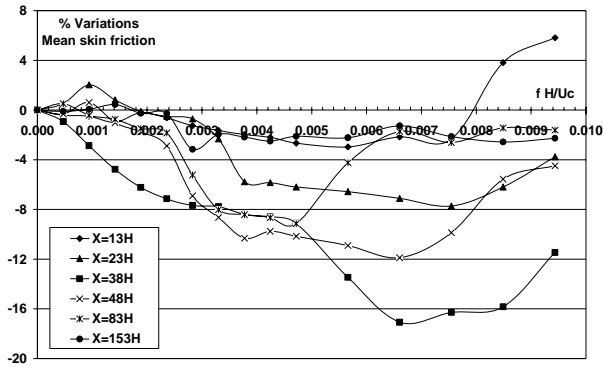
Fig. 9 Effect of forcing frequency. Mean skin friction percentage variations along the streamwise direction. Configuration $L_{1\ 3}$ R $_{4\ 6}$. Z=0.357B. Re_τ=370

The skin friction rms variations highlight roughly half reductions respect to those exhibited at the lower Reynolds number. Peak of attenuation equal to 5.24% is obtained at X=48H for fH/Uc=0.0045. As can be observed, also at higher Reynolds the effects of the forcing are persistent up to long distance from the injection section even if at a lower level of efficiency. For the two Reynolds numbers the highest drag reductions were obtained for two different synthetic jets array configurations and for two different dimensional frequencies. This fact can be related with the near wall structure that very near the wall is mainly characterised by the presence of very long streamwise organized structures, namely the low speed streaks, whose length in terms of wall units is equal to 1000 viscous length. Considering as characteristic length of the array, the distance

L_{car} between the centre of each active group of synthetic jets, the configurations $L_{1\ 5}$ R $_{6\ 10}$ and $L_{1\ 3}$ R $_{4\ 6}$ are characterised by lengths respectively equal to 25.8mm and 15.5mm.
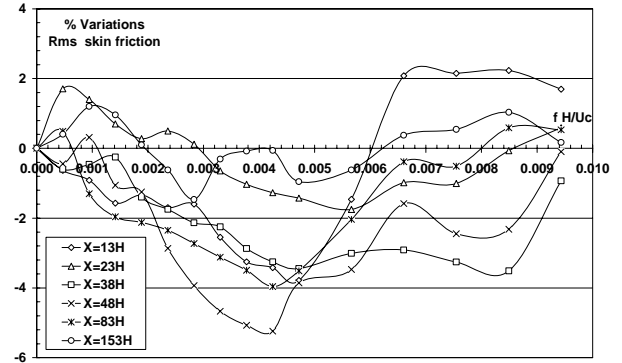
Fig. 10 Effect of forcing frequency. Rms skin friction percentage variations along the streamwise direction. Configuration $L_{1\ 3}$ R $_{4\ 6}$ Z=0.357B. Re_τ=370

In terms of wall units the two lengths are equivalent to 494 viscous length for Re_τ=180 and to 504 viscous length for Re_τ=370. The two configurations at the two Reynolds numbers give rise at the same characteristic non-dimensional length L_{car}^+ that is equal to half the typical low speed streaks length. The two forcing configurations appear tuned on the same typical length of the low speed streaks. Probably the forcing act as disrupting or weakening the low speed streaks that are mainly responsible for the origin of the quasi streamwise vortices that generate high values of the skin friction.

For each streamwise distance 13<X/H<153, measurements of the instantaneous wall shear stress in the spanwise direction were also performed on the wall corresponding to the same side of the synthetic jets array. The percentage reductions of the mean and the rms values were integrated in the spanwise direction for each streamwise location. In figure 11 and 12 these integrated percentage variations are reported for Reynolds number equal to 180 and Reynolds number equal to 370 respectively. As also evidenced from the previous results, the spanwise integrated reductions are more consistent for the lower Reynolds number. The effects of the forcing involve a large part of the channel wall surface in both directions, streamwise and spanwise.
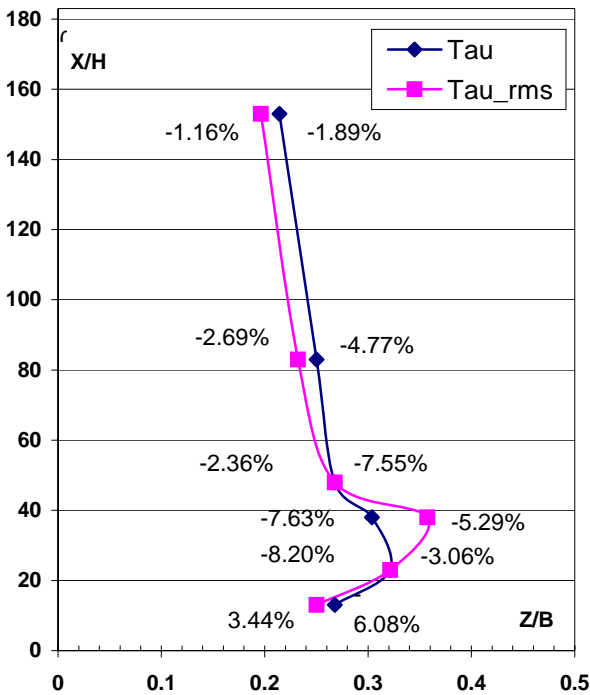
Fig. 11 Integrated spanwise percentage variations for $Re_\tau=180$. Configuration $L_{1\,5}\,R_{6\,10}$.

As the downstream locations are approached, the disturb propagate in spanwise direction toward the centre of the channel for both Reynolds numbers. The disturb seems penetrate more in the spanwise direction up to Z=0.18B in correspondence of X=153H at higher Reynolds number.

The influence of the forcing on the pressure gradient in the channel was also investigated measuring the static pressure distributions along the channel for Z=0.357B in the test section. In figure 13 the percentage variations of the pressure gradient dp/dx is displayed as function of the non-dimensional forcing frequency, for both Reynolds numbers and for the selected synthetic jets array configurations. The pressure distributions, not shown in the paper, also in forced conditions evidenced linear distributions. The results of figure 13 are in good agreement with those of figures 12 and figure 11 considering that the pressure gradients were only measured for Z=0.357B and the results of figure 11 and 12 are instead spanwise integrated variations.

Figure 13 shows how the forcing is more efficient at lower Reynolds number and the

percentage variation of the pressure gradient exhibits maximum reduction, as it was expected, for the same forcing frequency related with the results of figure 3.
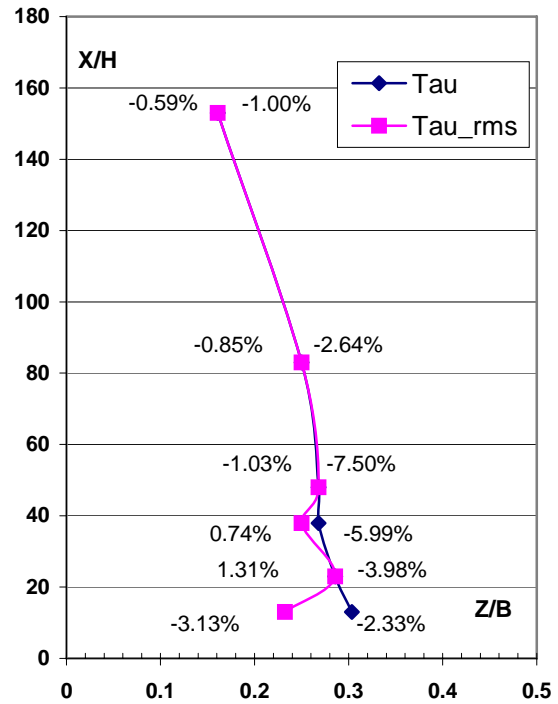
Fig. 12 Integrated spanwise percentage variations for $Re_\tau=370$. Configuration $L_{1\,3}\,R_{4\,6}$.
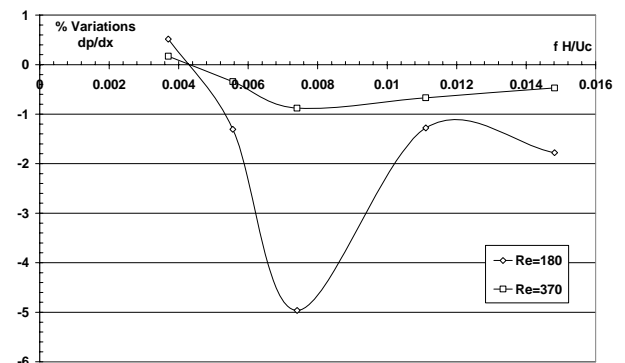
Fig. 13 Percentage variations of pressure gradient for $Re_\tau=180$ and $Re_\tau=370$. Z=0.357B

The spectra of the wall shear stress fluctuations at different streamwise and spanwise location for both Reynolds numbers were evaluated. In figure 14 an example of spectra for X=38H, $Re_\tau=180$ and $Re_\tau=370$ are presented in natural and forced conditions.

7
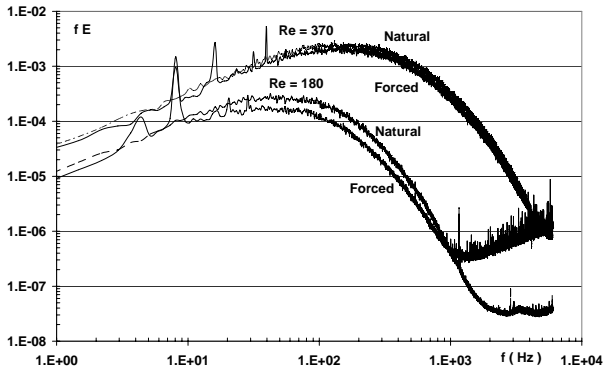
Fig. 14 Energy spectra. $Re_\tau=180$ and $Re_\tau=370$. X=38H. Z=0.357B.

Fig. 15 Autocorrelation function of the skin friction fluctuations. $Re_\tau=180$ and $Re_\tau=370$. X=38H. Z=0.357B

The energy spectra in the forced cases are characterized by lower levels of energy over the whole range of frequencies for both Reynolds numbers. Higher energy attenuations are present for $Re_\tau=180$ especially in the intermediate range of frequencies (10< f <500 Hz). Peaks of concentrated energy dominate the spectra in correspondence of the forcing frequency and higher harmonics for both Reynolds numbers. Specifically, energy peaks are centred at f=4Hz for $Re_\tau=180$ and at f=8Hz for $Re_\tau=370$. Moreover the spectra also exhibit a shifting of the energy distributions towards the low frequency range in the forced conditions, in particular for the lower Reynolds number. These spectra characteristics are evident also at all the streamwise distances even at the highest distance X=153H. The presence in the spectra of the energy peak could be interpreted as a global channel flow oscillation at the same forcing frequency. Moreover also other interpretations can be possible. An organized flow structure originating from the interaction could probably evolve in the channel, oscillating at the same forcing frequency. In figure 15 the autocorrelation function of the wall shear stress fluctuations is reported in the natural and forced conditions. The time delay is made dimensionless through the viscous time of natural cases corresponding to $Re_\tau=180$ and $Re_\tau=370$.

The dimensionless times of macroscale T^+ for each case analysed has been also evaluated calculating the area under the curves of autocorrelation functions.

In figure 15 the values of T^+ are also shown. As can be observed for both Reynolds numbers the curves corresponding to the natural cases are almost coincident evidencing a macroscale time equal to $T^+\approx20$. The curves corresponding to the forced cases are both characterised by higher values of the autocorrelation function especially for the lower Reynolds number. The time of macroscale is increased more than 50% in the forced conditions respect to the natural case for $Re_\tau=180$. The increasing of the macroscale time is typical of many controlled flows that exhibit drag reduction and it is mainly attributed to the aggregations or/and growing of the near wall structures.

Near wall events were also identified applying VITA techniques to the skin friction time series. The time of averaging for the evaluation of the local variance was kept equal to 13 viscous times while the threshold level k was fixed to one as proposed by Saha and Antonia [14]. Only accelerated events $d\tau_w/dt >0$ was identified for different streamwise and spanwise positions. In figure 16 the percentage variations of VITA events along the channel, for Z=0.357B are displayed.

For both channel flow conditions and for 13<X/H<153, reductions of VITA accelerated events are present. In particular for $Re_\tau=180$ in the range $23\le X/H \le83$ the maximum reduction of events is equal to 23% and is positioned at X/H=48. Also for the higher Reynolds number in the range 13<X/H<153 the channel flow is characterised by lower number of VITA events

respect to the natural case. Nevertheless the amount of the reduction is lower respect to that of lower Reynolds number.
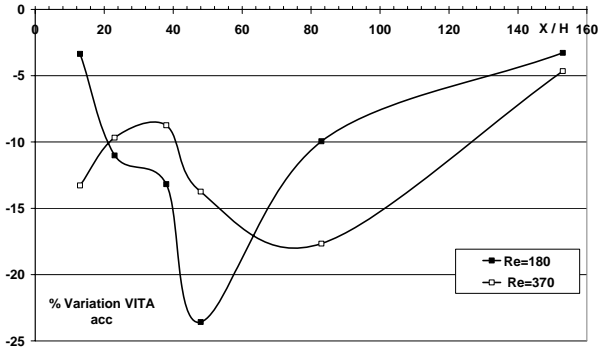
Fig. 16 Percentage variations of VITA accelerated event of the skin friction fluctuations. Re$_\tau$=180 and Re$_\tau$=370. Z=0.357B

VITA events are the evidence of near wall dynamics due to the bursting phenomenon that takes place as a consequence of rapid ejection of fluid that determine turbulence production. The fact that the number of VITA events are reduced in the forced flow should be related with the effects of the forcing on the near wall dynamics. In particular, as anticipated, the forcing could weaken the near wall dominant structures giving rise to attenuated interactions and at reduced turbulent kinetic energy production. The percentage variations of the rms values of the skin friction fluctuations corresponding to the same conditions of the results reported in figure 16, are reported in figure 17.

The correspondence between the reduced number of events and the reduced wall turbulence fluctuations is evident for both Reynolds numbers. As for the VITA events reductions, also the rms percentage variations display a range of X/H where the maximum reduction appear. At lower Reynolds number higher attenuations of turbulent fluctuations are present respect to that of the higher Reynolds number.
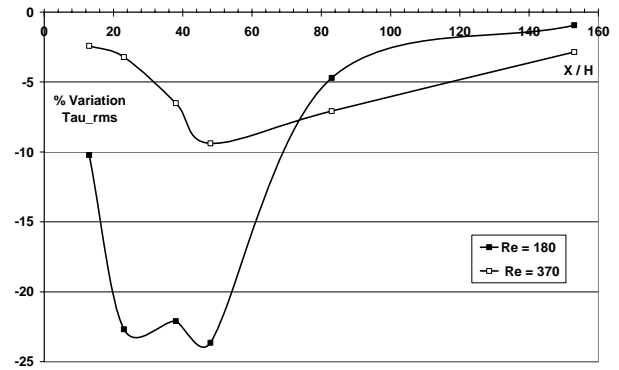
Fig. 17 Percentage variations of rms values of the skin friction fluctuations. Re$_\tau$=180 and Re$_\tau$=370. Z=0.357B

4 Conclusions

Two arrays of adjacent synthetic jets aligned in the streamwise direction have been used to force transversally a fully developed turbulent channel flow. The effect of the forcing frequency and of the arrays configuration have been exploited for two different Reynolds numbers. For appropriate array configuration and for nearly the same range of non-dimensional forcing frequency (f H / U$_c$) at both Reynolds number have been observed drag reduction and wall turbulent fluctuations attenuations. Much higher reductions are evidenced at the lower Reynolds number of the order of 22% for the mean wall shear stress and of 9% for the skin friction fluctuations. The effects of the transversal forcing are persistent up to long distances (X=153H) downstream the injection section and penetrate in the spanwise direction up to Z=0.22B for Re$_\tau$=180 and up to Z=0.18B for Re$_\tau$=370.

Modifications of the wall structure take place under the effects of the forcing as showed by energy spectra, autocorrelation function and VITA accelerated events that reveal great difference respect to the natural case especially at the lower Reynolds number. In particular in the forced conditions, energy spectra of wall shear stress exhibit lower levels of energy over a large range of frequencies showing a shifting towards the low frequency range. The autocorrelation function highlight higher values in the controlled case, evidencing higher time of macroscale.

References

[1] Jung W., Mangiavacchi N., Akhavan R. Suppression of turbulence in wall-bounded flows by high-frequency spanwise oscillations. *Phys. Fluids* A, Vol. 4, No. 8, pp. 1605, 1992.

[2] Laadhari, F., Skandaji, L. and Morel, R. Turbulence reduction in a boundary layer by a local spanwise oscillating surface. *Phys. Fluids,* Vol. 6, No. 10, pp. 3218-3220, 1994.

[3] Choi, K. S., DeBisschop, L. and Clayton, B.R. Turbulent boundary layer control by means of spanwise wall oscillations. *AIAA J*, Vol. 36, pp. 1157-1163, 1998.

[4] Choi, K.S. Near-wall structure of turbulent boundary layer with spanwise-wall oscillation. *Phys. Fluids* Vol. 14, pp. 2530, 2002.

[5] Iuso, G., Di Cicca, G. M., Onorato, M., Spazzini P.G. and Malvano R. Velocity streak structure modifications induced by flow manipulation. *Phys. Fluids* Vol. 15, pp. 2602, 2003.

[6] Du, Y, and Karniadakis, G. E. Suppressing wall-turbulence via a transverse travelling wave. *Science* Vol. 288, pp. 1230-34, 2000.

[7] Du, Y, Symeonidis, V and Karniadakis, G. E. Drag reduction in wall- bounded turbulence via a transverse travelling wave. *J. Fluid Mech*. Vol. 457, pp. 1-34, 2002.

[8] T. W. Berger, J. Kim, C. Lee, and J. Lim, Turbulent boundary layer control utilizing the Lorentz force. *Phys. Fluids* Vol. 12, pp. 631-49, 2000.

[9] Karniadakis G., Choi K.S., Mechanisms on transverse motions in turbulent wall flows. *Ann. Rev. Fluid Mech.* Vol. 35, pp. 45, 2003.

[10] L.Smith and A.Glezer , The formation and evolution of synthetic jets. *Phys. Fluids*, Vol. 10, pp. 2281, 1998.

[11] A.Glezer and M.Amitay. Synthetic jets. *Ann.Rev.Fluid Mech* Vol. 34, pp. 503, 2002.

[12] Park, Y.D., Park,S.H. and Sung, H.J. Measurement of local forcing in a turbulent boundary layer. *5th International Symposium on Particle Image Velocimetry Busan, Korea*, September 22-24, 2003.

[13] Iuso, G. and Di Cicca G.M. Interaction of synthetic jets with a fully developed turbulent channel flow. *Journal of Turbulenc*, Vol.8, No. 11, 2007.

[14] Saha,D.A. and Antonia, R.A. Scaling of wall shear stress fluctuations in a turbulent duct flow. *AIAA J.*, Vol. 25, pp.25-29, 1987.